# Acetone fraction measurements in bicomponent evaporating droplets using laser-induced fluorescence

C. Maqua, V. Deprédurand, G. Castanet, F. Lemoine*
LEMTA, Nancy-Université, CNRS
2, Avenue de la forêt de Haye, BP 160,
54504 Vandoeuvre-lès-Nancy, France

**Abstract**
Commercial fuels are complex mixtures, the evaporation of which remains particularly difficult to model. In this paper, the evaporation of binary droplets made of ethyl-alcohol and acetone is investigated using a technique of measurement of the droplet composition developed in purpose. This technique exploits the laser induced fluorescence of acetone which acts as a fluorescent tracer as well as the more volatile component of the fuel, associated with an accurate measurement of the droplet diameter using forward scattering interferometry. A model of the fluorescence intensity of the binary mixture, taking into account the absorption of the acetone molecules, is proposed and validated. Finally, the technique is demonstrated on binary combusting droplets in linear stream.

## 1. Introduction

Multicomponent droplets evaporation is a critical issue for the design of modern combustors. In particular, an improvement of the knowledge of multicomponent droplets vaporization process is necessary, especially when each component evaporates at different boiling temperatures. Fuel composition significantly influences local fuel-air ratio and therefore, ignition delays and pollutant emissions. Due to the complexity of the different phenomena involved in the heating and evaporation phases of the droplet, the models must be validated through elementary experiments, such as monodisperse droplet streams. Simplified representative fuels are also used since real fuels are composed of hundreds of molecular species. Evaporation of bicomponent droplets made of mixtures of acetone and ethanol are also considered in the present study. The aim is to develop an instantaneous measurement technique of the acetone fraction in the droplets, based on laser induced fluorescence of acetone, induced by a UV laser radiation at 266 nm. In this experiment, acetone acts as a fluorescent tracer as well as the more volatile component of the fuel. The technique was applied to the characterization of the acetone fraction of bicomponant droplets evaporating in a flame produced by previously injected combusting droplets in linear stream.

## 2. Experimental facilities facilities

A linear monodisperse droplet stream is generated by Rayleigh disintegration of a liquid jet which experiences a mechanical vibration provided by a piezoceramic ([1], ([2] and [3]). A laminar spray flame is ignited by means of an electrically heated coil, placed just after the break-up zone of the liquid jet (figure 1). In such a configuration of stream, the dimensionless spacing parameter $C$ is defined as the ratio between the droplet spacing $L$ and the droplet diameter $D$ ($C = L/D$).

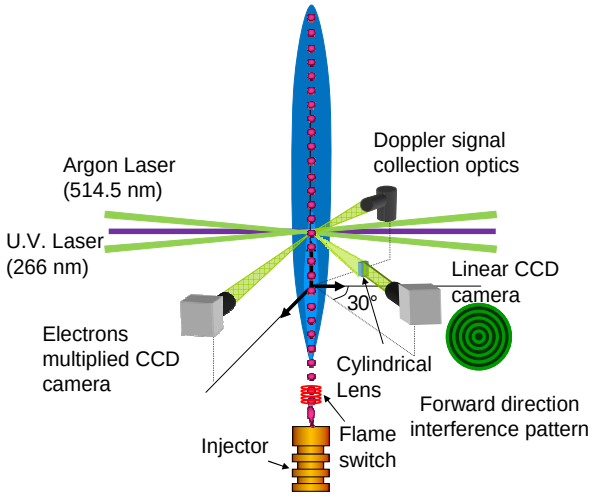


*Figure 1: Sketch of a combusting monodisperse droplet stream with the droplet diameter measurement facilities.*

Knowledge of the droplet size reduction is necessary to characterize the evaporation of the droplets. The measurement technique is based on the interaction between a spherical droplet and a laser beam [4]. A beam issuing from an argon ion laser is focused on a droplet (figure 1). Interferences between reflected rays and one time refracted rays are generated in the forward direction. The high frequency of the droplets passage

* Corresponding author: fabrice.lemoine@ensem.inpl-nancy.fr
Associated Web site: http://www.ensem.inpl-nancy.fr/LEMTA/
Proceedings of the 21th ILASS - Europe Meeting 2007

makes that the fringe pattern appears stationary. Measurement of the angular interfringe near the forward scattering angle of 30° enables to determine the droplet diameter within ±0.5 µm with a very limited sensitivity to the droplet refractive index [5].The interference pattern is focused in one direction by means of a cylindrical lens in order to increase the light power density. Image of the spatial intensity distribution is formed on the linear sensor chipset of a CCD camera (4096 pixels). The angular interfringe is measured between two interference maxima in order to derive the droplet size as suggested by Frohn and Roth [6]. The droplet velocity is measured simultaneously by an additional LDA system. With the help of the droplet velocity, distance from the injector exit can be converted easily into time.

### 3. Fluorescence of acetone droplets

In the present experiment, acetone acts as an evaporating fuel as well as a fluorescent tracer for the liquid phase. . In a bicomponent mixture, one of the components (acetone in the present case) can be excited to fluoresce. The total emitted fluorescence can be used as a measurement of the number of molecules of the fluorescing component. In a monodisperse droplet stream and with the use of an independent and accurate measurement of the droplet diameter, this information can be used to derive the relative concentration of the fluorescing component in the droplet.

The absorption of liquid acetone is very efficient at 266 nm which corresponds to the radiation of a quadrupled Nd-Yag laser (Figure 2). The resulting fluorescence spectrum is broadband with a maximum emission in the 420-520 nm region (figure 2). It was decided to detect the fluorescence on a narrow spectral band centered at 450 nm (bandwidth $\Delta\lambda$=20 nm) to avoid any residual radiation of the 2nd harmonic of the Nd-Yag laser at 532 nm.

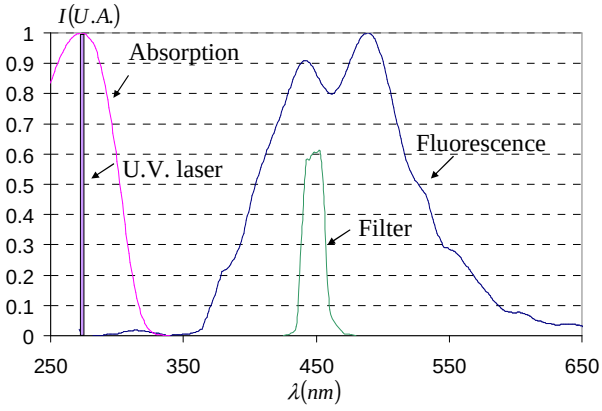


*Figure 2: absorption and fluorescence spectra of liquid acetone (fluorescence is induced by the quadrupled Nd-Yag UV laser radiation at 266 nm).*

LIF results from a process that begins with the absorption of the incident light by the acetone molecules which are promoted to a higher energy level. Some of the excited molecules return to the ground state by emitting fluorescence. The intensity of the fluorescence signal, collected from an elementary volume *dV*, assuming no saturation, is given by [7]:

$$dI = K_{opt} E_l dV C_a \varepsilon_a \eta \qquad (1)$$

where $K_{opt}$ is a constant specific to the optical device, $E_l$ is the local incident laser energy per pulse per unit area, $C_a$ is the molecular concentration of the absorbers, i.e. acetone molecules. $\varepsilon_a$ ($mol^{-1}.l.m^{-1}$) is the molar absorption coefficient for the acetone molecule at 266 nm and $\eta$ *is* the fluorescence quantum yield of acetone and takes into account all non radiative decay processes including collisionnal quenching. The optical constant $K_{opt}$ can then be evaluated using a suitable reference. It depends on experimental parameters such as probe volume, solid angle, spectral and spatial efficiencies of filters and detection devices. The local intensity $E_l$ can be related to the laser incident intensity $E_0$ by the Beer's absorption law ( $E_l = E_0 e^{-\varepsilon_a C_a x}$, where *x* is the optical path of the incident laser beam).

In the present study, the case of a droplet completely illuminated by a plane wave will be examined. The probe volume *V* is therefore replaced by the droplet volume $V_d$ in eq.(1). To evaluate the local excitation energy $E_l$ in the droplet, the focusing effect of the spherical interface and the noticeable absorption must be taken into account. The absorption, depending on the droplet diameter and acetone fraction, tends to decrease the efficiency of the excitation by the incident laser beam. In a mixture of ethanol and acetone, acetone fluorescence can be quenched by both fluorescence by both acetone and ethanol molecule. By using the usual definitions of the quenching terms ([7] and [8]), neglecting the radiative decay rate in comparison to decay by quenching, the term $C_a\eta$ can be rewritten:

$$C_a \eta \propto \frac{\chi_a}{\chi_a \mu + 1} \qquad (2)$$

where $\chi_a$ is the molar fraction of acetone and $\mu$ is a dimensionless empirical constants, which was properly calibrated ( $\mu \approx 1.15$ ) by measuring the fluorescence intensity for different acetone fractions in the mixture. After collection all over the droplet volume, the fluorescence signal is expressed by:

$$I = K_{opt} K_{spec} \frac{\chi_a}{\chi_a \mu + 1} V_d E_0 \xi(\chi_a, D) \qquad (3)$$

where $\xi(\chi_a, D)$ is the efficiency of the laser excitation which can be defined, according to the following expression:

$$\xi(\chi_a, D) = \frac{\int_{V_d} E(x, y, z, \chi_a, D)}{\int_{V_d} E(x, y, z, \chi_a = 0, D)} \qquad (4)$$

$E(x, y, z, \chi_a, D)$ is the internal energy field at given acetone fraction $\chi_a$ and droplet diameter *D* and $E(x, y, z, \chi_a = 0, D)$ is the same quantity assuming no absorption. The internal field can be calculated by a ray

tracing method using the 3D Snell's law at the droplet interface and taking into account the absorption along the ray path according to Beer's absorption law.

The fluorescence intensity was computed in order to evaluate its sensitivity to a variation of the acetone volume fraction. The predicted evolution of the fluorescence intensity as a function of the acetone fraction is presented in figure 3 for different droplet diameters. As expected, the fluorescence intensity exhibits a pronounced dependence on the droplet diameter. Additionally, for a given droplet diameter, the variation of the fluorescence intensity with the acetone fraction is very steep for the lowest acetone fractions. A quasi-linear region can be pointed out with an upper limit at $Z_a$=0.1. The sensitivity to acetone fraction begins to decrease after $Z_a$=0.1, but remains noticeable up to $Z_a$=0.3 for droplets of about 100 µm in diameter. For acetone fractions higher than 0.3, the sensitivity is very limited. This can be attributed to the balance between the increase of the acetone fraction and the resulting extinction of the incident laser beam by absorption, which reduces the fraction of the droplet volume that contributes to the fluorescence signal. The moderate decrease of the fluorescence intensity for the acetone fractions higher than $Z_a$=0.3 can be explained by the correction of the quenching term with the fuel composition. This correction tends to decrease the fluorescence efficiency for increasing acetone fractions.

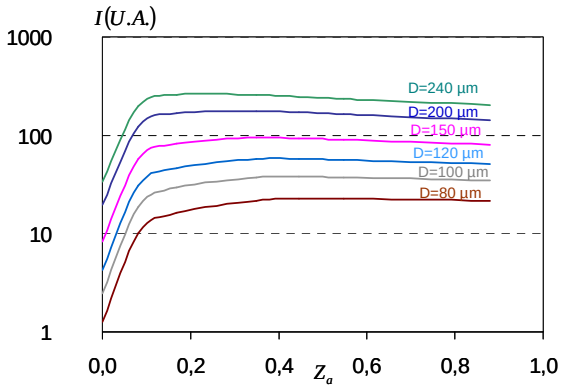


*Figure 3: Calculated evolution of the fluorescence intensity as a function of the acetone volume fraction for different droplet diameters.*

## 4. Experimental set-up and data reduction

In the present experimental setup, the full aperture of the laser beam (9 mm at $1/e^2$) is used to induce the fluorescence of the droplets. The fluorescence is acquired on the array detector of an electron multiplier CCD camera, equipped with a high magnification objective. The fluorescence signal detected by the camera is digitalized on 14 bits i.e. 16384 grey levels. The laser shot is triggered on the piezoceramic frequency at which the droplets are generated. A phase shifter allows adapting the trigger frequency to take into account the time delay due to the displacement of the droplets from the injector exit to the measurement position. The camera acquisition is triggered on the laser pulse. The camera is equipped with the already used band pass interference filter to isolate a spectral band of the fluorescence signal A sample of the laser beam is deviated in order to measure the energy per pulse by means of a pyroelectric detector. The energy measurement is done synchronously with the image acquisition by the CCD camera, in order to normalize the fluorescence intensity by the incident energy and to account for the pulse to pulse variation of the laser energy (figure 4).

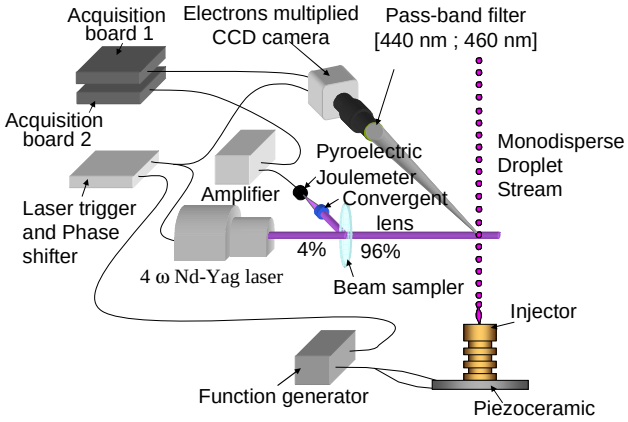


*Figure 4: Block diagram of the measurement layout.*

When the spaced-averaged composition of the droplets is wished, a region of interest is defined within the images and includes several droplets (3 or 4). The images resulting of 200 laser shots are normalized by the energy of each laser pulse and after subtraction of the background noise the signal is averaged over all the images and over the region of interest.

An example of image acquisition is given in figure 5 for two droplet diameters, $D$=109 µm and $D$=187 µm associated with the acetone fractions $Z_a$=0.2 and $Z_a$=0.9 respectively. The experimental images were compared to the results of the numerical simulation with the 3D ray tracing code, taking into account the observation angle of the CCD camera. The images are featured by the strong absorption of the acetone and the good agreement between the experimental and calculated intensity maps can be noticed.

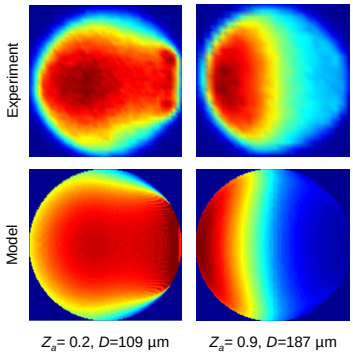


*Figure 5: Excitation field within the droplet (left: calculation by ray tracing; right: experiment).*

## 5. Experimental results

### 5.1. Validation of the fluorescence model

- Influence of the droplet diameter

Several droplets sizes were generated by tuning the frequency of the piezoceramic of the monodisperse droplet generator. Data were collected for different droplet diameters (from 80 µm to 132 µm) and for two acetone fractions ($Z_a$=0.1 and $Z_a$=0.2). The measurements were performed after formation of the spherical droplets, but sufficiently close to the injector exit, to neglect evaporation and subsequent variations in the acetone fraction. Furthermore, as the droplet trajectories are very stable close to the injector exit, the droplets are exposed to the same profile of energy when they cross the laser beam. The evolution of the fluorescence intensity as a function of the droplet diameter is presented in figure 6 for the two acetone fractions. As expected the fluorescence intensity increases with the droplet diameter and with the acetone volume fraction. Here also, a good agreement with the fluorescence model is observed in the investigated size range.

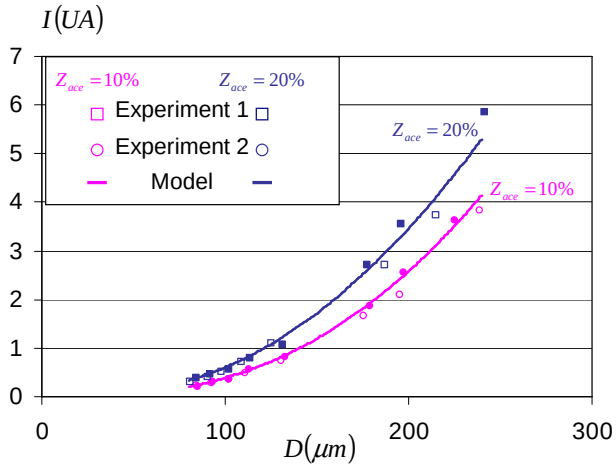


*Figure 6: Measurements of the fluorescence intensity as a function of the droplet diameter for Za=0.1 and Za=0.2. Comparison to the model.*

- Influence of the acetone fraction

The influence of the acetone fraction was also tested for three droplet diameters ($D$=90 µm, $D$=150 µm and $D$=200 µm) and three acetone fractions ($Za_0$=0.05, $Za_0$=0.1 and $Za_0$=0.2) (figure 7). The evolution of the fluorescence intensity is presented as a function of the acetone fraction and for the three droplet diameters. The fluorescence model seems to follow the experimental evolution with a rather good accuracy in the investigated range of acetone fraction. Nevertheless, the discrepancy of measurements with the model seems more pronounced for the biggest droplets, which may be due to possible non-spherical droplets.

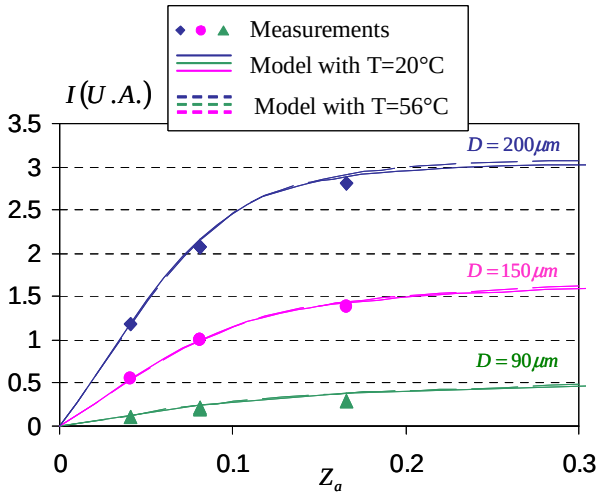


*Figure 7: Measurements of the fluorescence intensity as a function of the acetone fraction for three droplet diameters. Comparison to the model.*

### 5.2. Composition measurements in combusting droplets

- Measurement process

In measurement conditions, the trajectories of the droplets in the laser beam may be not perfectly steady due to some turbulence that can be generated by the flame. This affects the fluorescence signal since the distribution of the energy in the laser beam is not homogeneous. In order to reduce the statistical bias induced by these unwanted effects, it is preferred to do the averaging of the fluorescence signal over a region of interest containing 4 droplets, i.e 1.5 mm in high.

In combustion experiments, the reference measurement is previously taken close to the nozzle exit, when the droplets are formed, without any flame. The reference diameter $D_0$ is determined by using the measured injected flowrate $Q$ and the piezoceramic frequency $f$ ( $D_0 = (6Q/\pi f)^{1/3}$ ). Since the composition is supposed to be well known at this point (i.e. equal to the initial composition), the optical and spectroscopic constants can be eliminated and the acetone fraction is then derived from:

$$\frac{I^*}{I_0^*} = \frac{\chi_a}{\chi_a \mu + 1} \frac{\chi_{a_0} \mu + 1}{\chi_{a_0}} \frac{V_d \xi(\chi_a, D)}{V_{d_0} \xi(\chi_{a_0}, D_0)} \qquad (5)$$

where $I^*$ denotes the fluorescence intensity normalized by the incident laser energy.

The determination of the acetone fraction required the inversion of eq. (5). This inversion is considerably eased by working with a 2D-interpolation of $\xi$ instead of running the heavy ray tracing code for any guest value of $\chi_a$. The interpolated function is obtained from a relatively dense meshing of the space ($\chi_a$,D).

- Results

Droplets with a diameter on the order of 100 µm were also considered in this study. Figure 8 depicts the variation of the fluorescence intensity with the distance from the nozzle exit for three initial compositions $Z_{a0}$=0.3, $Z_{a0}$=0.2 and $Z_{a0}$=0.1. The operating conditions are summarized in table 1. The initial diameters differ slightly for the three compositions since it was difficult to achieve perfectly steady droplet streams while maintaining the diameter. The droplet spacing $C$ is also added in table 1 and is almost identical for the three investigated conditions.

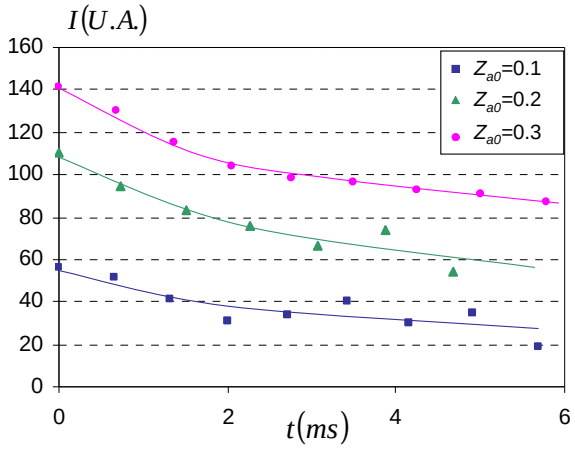


*Figure 8: Temporal evolution of the fluorescence intensity. Case of combusting monodisperse droplets streams ($Za_0$=0.1; $D_0$=95.3 µm, $Za_0$=0.2; $D_0$=99.5 µm and $Za_0$=0.3 $D_0$=97.9 µm).*

| $D_0$ (µm) | 95.3 | 99.5 | 97.9 |
|---|---|---|---|
| $Z_{a0}$ | 0.1 | 0.2 | 0.3 |
| **C** | 3.18 | 3.07 | 3.17 |
| $a_{eff}$ (m²/s) | $3.9.10^{-9}$ | $4.3.10^{-9}$ | $4.9.10^{-9}$ |

*Table 1: Operating conditions.*

Distance from the injector exit was converted into time by means of the local droplet velocity measured by LDA. The origin time is taken at the exit of the ignition device. As expected, the fluorescence intensity decreases with the time elapsed from the injection. This decrease comes from the preferential depletion of acetone, which is the more volatile component in the mixture. The temporal evolution of the droplet diameter is presented in figure 9. The droplet shrinkage seems to follow a $D^2$ law [9]. A perfect sphericity is required for the size measurement but is difficult to insure shortly after the break-up. For this reason, size measurements don't start exactly at the same distance from the injector exit depending on the tested conditions. The acetone volume fraction can be inferred from the measured fluorescence intensity according to eq. (5). The temporal evolution of the acetone volume fraction is shown in figure 10. The first measurement point at $t$=0 corresponds to the injection conditions. The depletion of acetone is the quickest at the beginning of the evaporation then it slows down considerably in a second phase. Initially, the droplets are rather cold and only acetone evaporates significantly. Then, since the droplets are heated up, ethanol begins to participate increasingly to the vaporisation flowrate. With the rather strong initial vaporization of acetone, ethanol becomes extremely in excess near the surface of the droplet, even if the saturation pressure of ethanol is much lower than the one of acetone. According to the Raoult's law, at the liquid/vapour interface of an ideal mixture, the molar fraction of the vapour of each component is proportional to their liquid fraction. For this reason, the vaporisation rate of ethanol increases whereas the one of acetone slows down which ultimately results in a stagnation of the space-averaged acetone fraction (phase 2). The whole acetone present in the core of the droplet must diffuse to the surface of the droplet before that the surface temperature can get higher than the boiling temperature of acetone and the vaporization rate of ethanol increases further again. To compare safely the evolutions of the previous droplets streams, the results are put in a dimensionless form. The time is normalized by the acetone diffusion time $D^2/a_{eff}$, where $a_{eff}$ is the effective diffusivity depending on the droplet Peclet number as defined by Abramzon and Sirignano [10], whereas the acetone volume fraction is divided by its initial value. The values of $a_{eff}$ are quoted in table 1. As expected, the normalized volume fraction of acetone (figure 11) seems to follow the same trend regardless to the initial conditions, i.e. the composition and the droplet diameter. The more scattered points are for the case $Za_0$=0.1, for which the relative uncertainty is the largest.

Taking into account all the uncertainties sources, including diameter, florescence intensity, absorption coefficient of acetone and empirical constant $\mu$, the uncertainty $\Delta Z_a$ is respectively $\pm 0.85\%$ for $Z_{a_0}$=10%, $\pm 1\%$ for $Z_{a_0}$=20% and $\pm 2.1\%$ for $Z_{a_0}$=30%.

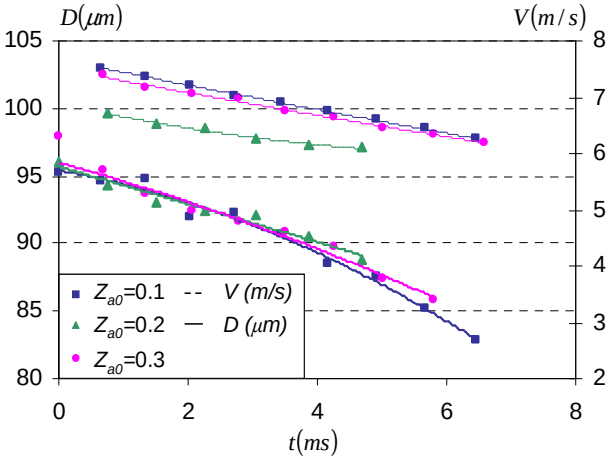


*Figure 9: Temporal evolution of the raw and squared diameters measured for $Za_0$=0.1, $Za_0$=0.2 and $Za_0$=0.3.*

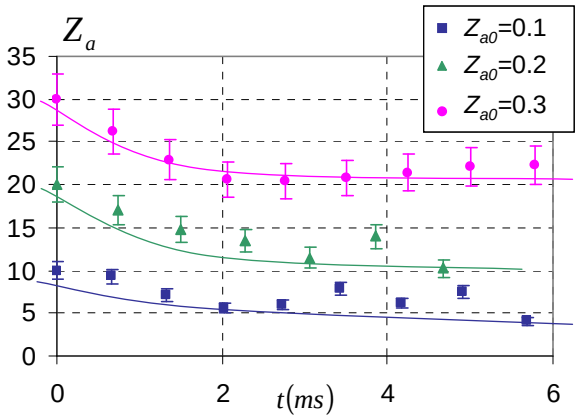


*Figure 10: Measured evolution of the acetone volume fraction as a function of time ($Za_0$=0.1, $Za_0$=0.2 and $Za_0$=0.3).*

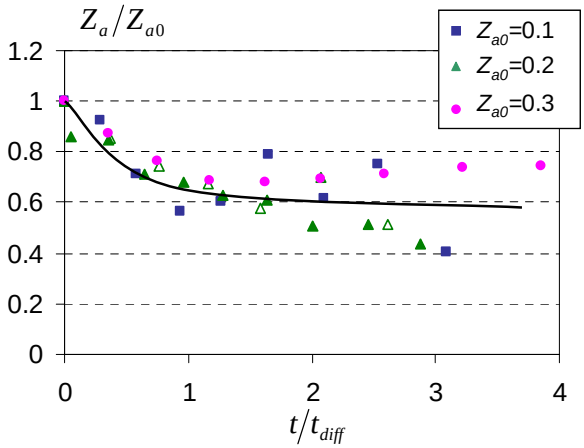


*Figure 11: Evolution of the normalized acetone volume fraction as a function of the dimensionless time for $Za_0$=0.1, $Za_0$=0.2 and $Za_0$=0.3.*

## 6. Conclusion

This paper presents one of the first attempts to measure the transient evolution of the composition of binary droplets. The composition is based on direct measurements of the fluorescence signal of acetone which acts also as a volatile fuel in the mixture and an accurate independent measurement of the droplet diameter. The fluorescence is induced by an UV laser at 266 nm. The technique is sensitive to the composition variations when the acetone volume fraction is less than 0.3. Above this value, the strong absorption of acetone molecules becomes a serious disadvantage. The technique accuracy is of the order of 2% in term of acetone volume fraction.

To implement the technique, one of the limitations comes from the fact that the volume fraction is inferred directly from the intensities, which implies a strict controlled of the operating conditions.

In future, these experimental data will be used to assess multicomponent evaporation models taking into account the diffusion within the droplets. acetone fraction gradients on the measurements.

**Acknowledgement:** This program has been conducted in the framework of the ASTRA program, supported by CNRS and ONERA.

## References

1. P. Lavieille, F. Lemoine, G. Lavergne, M. Lebouché, Evaporating and combusting droplet temperature measurements using two-color laser-induced fluorescence, *Exp. in fluids*, 31: 45-55, 2001

2. P. Lavieille, F. Lemoine, M. Lebouché, Experimental investigation on interacting low evaporating droplets temperature in linear stream using two colors laser induced fluorescence, *Combustion Science and Technology* , 174 (4): 117-142, 2002.

3. G. Castanet, M. Lebouché, F. Lemoine, Heat and mass transfer characterization in combusting monodisperse droplets in linear stream, *Int. J. Heat and Mass Transfer*, 48: 3261-3275, 2005.

4. G. Koenig, K. Anders, A. Frohn, A new light scattering technique to measure droplet diameter of periodically generated moving droplets, *J. Aerosol Sci.*, 17: 157-167, 1986.

5. P. Massoli, Rainbow refractometry applied to radially inhomogeneous spheres : the critical case of evaporating droplets, *Applied Optics*, 37: 3227-3235, 1998.

6. A. Frohn, N. Roth, Dynamics of droplets, Sringer Verlag, *Heidelberg*, Germany, 1998.

7. F. Lemoine, Y. Antoine, M Wolff, M. Lebouché, Simultaneous temperature and 2D velocity measurements in a turbulent heated jet using combined laser-induced fluorescence and LDA, *Exp. in Fluids*, 26: 315-323, 1999.

8. J. Glowacki, Further investigations into fluorescence quenching of the dyes by neutral salts, *Acta Physica Polonica*, 15: 767-780, 1964.

9. K. Kuo, Principles of combustion, John Willey & sons, Inc., *New Jersey*, USA, 2005.

10. B. Abramzon, W. A. Sirignano, Droplet vaporization model for spray combustion calculations, *International Journal of Heat and Mass Transfer*, 32: 1605-1618, 1989.